(Meth)acrylate liquid crystalline polymers for membrane applications

Feras Rabie,[1] Zdenka Sedlakova,[2] Swapnil Sheth,[1] Eva Marand,[1] Stephen M. Martin,[1] Lenka Poláková[2]

[1]Department of Chemical Engineering, Virginia Tech, Blacksburg, Virginia 24061
[2]Institute of Macromolecular Chemistry, Academy of Sciences of the Czech Republic, Heyrovský Sq. 2, 162 06, Czech Republic
Correspondence to: L. Poláková (E-mail: polakova@imc.cas.cz)

ABSTRACT: Synthesis and characterization of a series of linear copolymers with liquid crystalline side chains is reported. Methacrylate monomers containing cyanobiphenyl as a mesogenic group were prepared. These monomers were then copolymerized with 2-ethylhexyl acrylate in varying molar ratios. The structure and composition of the monomers and corresponding polymers were determined by ^{1}H-NMR, elemental analysis and size-exclusion chromatography. Thermal properties of the polymers were studied using differential scanning calorimetry, polarized optical microscopy, and X-ray scattering techniques. Increasing mesogen content resulted in an increase of the glass transition temperature of the copolymers. In addition, above a threshold mesogen content the copolymers exhibited smectic mesophases. Using a solution casting technique, a membrane was fabricated to study single gas transport behaviors. Permeabilities, were in the order of $CO_2 >$ propylene $> O_2 > N_2 > CH_4 >$ propane. Diffusion coefficients correlated well to Lenard–Jones Diameter. © 2015 Wiley Periodicals, Inc. J. Appl. Polym. Sci. **2015**, *132*, 42694.

INTRODUCTION

Liquid crystals are known as the fourth state of matter. They represent a state of matter which is characteristic with the ordering of a solid and the mobility of a liquid.[1] Depending on the class of the liquid crystal, ordering can be a function of temperature, solvent, concentration of solution, electric or magnetic fields, shear flow, grooving of the substrate surface, as well as anchoring interactions.[2,3] Thermotropic liquid crystals are further classified as low molecular weight liquid crystals or polymer liquid crystals. Low molecular weight liquid crystals have rod-like molecular structures and a rigid long axis with strong dipoles. Polymer liquid crystals have flexible polymer backbones and rigid mesogens, either attached to the polymer with a comb-like structure (side-chain liquid crystals), or fully incorporated in the polymer backbone (main chain liquid crystals) and combination thereof.[4] In sidechain liquid crystal polymers mesomorphic phase behavior is strongly dependent on the decoupling of the polymer backbone from the polar mesogen by the incorporation of spacer alkane chains. A previous study showed that as the spacer length increases, a more well-ordered mesogenic phase is formed, due to the increased mobility the spacer grants the mesogen.[5] However, a further increase in chain length can plasticize the material and resulted in a decrease of mesogenic ordering.[6]

The permeation through nonporous, dense, liquid crystal polymer membranes follows a three-step solution diffusion mechanism. Penetrant gas or liquid molecules dissolve onto the face of the membrane (feed side), diffuse across the length of the membrane, due to a concentration gradient, and finally desorb from the permeate face of the membrane and enter the downstream low pressure side of the system. Research on liquid crystal polymer (LCP) membranes for commercial and industrial applications has been limited due to the rheological properties and difficulty in processing of side-chain and main chain LCPs. Several studies have investigated light gas transport properties in linear LCPs aiding in the understanding of the fundamental mechanisms of gas transport.[7–9] For example, Kawakami *et al.*[9] have shown that the overall permeability of an LC polysiloxane with side chain mesogenic groups was governed by an activated diffusion mechanism as has been observed in other glassy polymers. In addition, the solubility increased with increasing temperature above the T_g due to the increase sorption of the penetrant gas in the increasingly disordered liquid crystalline mesogens. Glowacki *et al.*[10] studied the photoswitchable effect on gas permeation using azobenzene mesogens by imbibing porous membranes with the small molecular weight liquid crystals. A sorption–diffusion behavior was observed for the impregnated liquid crystals. The liquid crystal composition can be chosen such that the LC phase is more permeable than the

isotropic or vice versa. Furthermore, Rao et al.[11] developed an LC/PDMS crosslinked membrane prepared by silicone–hydrogen addition reaction. Although the fabricated membranes did not exhibit LC behavior, it was found that the introduction of LC material increased the rigidity of the PDMS backbone and increased the free volume available for gas molecules. Permeability was found to increase up to 5.0 wt % LC content.

Unfortunately, heating linear LCP membranes above the glass transition (T_g) and into the LC or isotropic states increases polymer mobility, which results in an undesirable decrease in the loss and storage moduli.[12] This results in a decrease in membrane stability, resulting in an inability to withstand the pressure gradients used in gas separation applications. In situ free radical polymerization of certain LC monomers with a crosslinking agent can result in temperature independent 'form retaining' polymeric materials that also exhibit LC properties. For this reason, a crosslinkable LCP material is desirable for the production of stable LCP membranes. Crosslinked polysiloxane (PS) based LC elastomers have already been synthesized for membrane separation applications.[13] The preparation of these membranes requires the use of a precious metal catalyst, making it potentially too expensive for scale up. To our knowledge, there have been no reported crosslinked LCP materials that could be used to produce membranes in a cost-effective manner. In addition, the total academic findings are too thin and discontinuous to derive a clear and reasonable mechanism for transport through LCP films.

The use of a single reaction scheme to produce multiple LCPs with various mesogen types and nonmesogen comonomers allows for an efficient method to study their gas transport mechanism and to optimize LCP membranes for specific applications. Common synthetic routes, such as azocoupling, Williamson reaction and esterification, can be used for the preparation of a variety of mesogenic monomers. These routes can be applied to common precursors to allow control over both the mesogenic group and the spacer group. Free radical polymerization as a means of LCP membrane fabrication also allows for the introduction of nonmesogenic comonomers and the flexibility to control the ratios of the mesogenic monomer and the nonmesogenic comonomer. This provides control over phase transition temperatures (e.g., glass transition, mesophase, and isotropic), specific volumes, and interactions with permeating gases. This study was conducted to develop and characterize novel LC polymers that will be used to better understand the dependencies of gas transport through LCP membranes and to provide a preliminary study on gas transport through LC copolymer membranes.

Herein we present the preparation and characterization of a set of novel (meth)acrylate copolymers with cyanobiphenyl based mesogenic side chains, as depicted in Figure 1. We demonstrate the use of free radical polymerization as a means of producing a series of polymers with varying mesogen type and mesogen content and we investigate their effect on phase behavior. In addition, the transport of N_2, O_2, CH_4, CO_2, propane, and propylene through an LCP membrane are presented. The preparation and transport properties of crosslinked methacrylate LCP membranes will be addressed in a future paper.
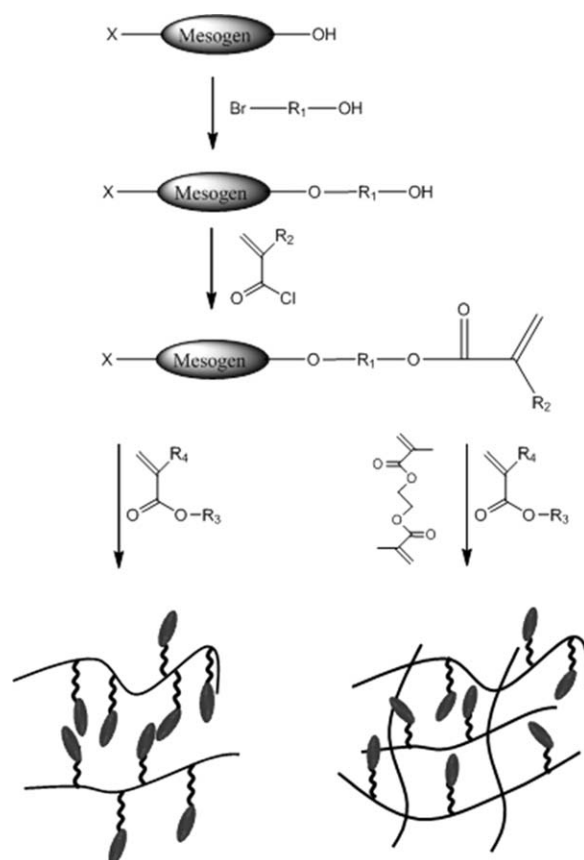

Figure 1. Scheme of the synthetic route for the preparation of linear (left) or crosslinked (right) liquid crystal polymers.

MATERIALS

11-bromo-1-undecanol (m.p. 46°C, Sigma Aldrich), sodium nitrite (Sigma Aldrich), sodium hydroxide (VWR), triethylamine (b.p. 89°C, VWR), toluene, heptane, ethanol and chloroform were used as received. Methacryloyl chloride (b.p. 96°C) and 2-ethylhexyl acrylate (b.p. 91°C/13 mbar) were distilled under vacuum prior to use. Acetone (HPLC grade) was dried using as received calcium carbonate. Potassium carbonate (VWR) and anhydrous calcium chloride were annealed for several hours prior to use. 2,2′-azobisisobutyronitrile (m.p. 103°C, Sigma Aldrich) was recrystallized with methanol several times prior to use.

METHODS OF MEASUREMENTS

^{1}H-NMR and elemental analysis were used to determine the structure and composition of the low-molecular weight and polymeric compounds. ^{1}H-NMR spectroscopy was performed at 300 MHz using deuterated chloroform ($CDCl_3$) as the solvent. Molecular weights of the synthesized polymers and their distributions were estimated using size-exclusion chromatography (SEC) with poly(methyl methacrylate) as a standard.

Thermal behavior of the copolymers was determined using differential scanning calorimetry (DSC). Measurements were performed using a Perkin Elmer DSC-2 instrument. The sample was first cooled to −50°C or −70°C and then heated to a temperature of 150°C, at a rate of 10°C/min. Liquid crystalline
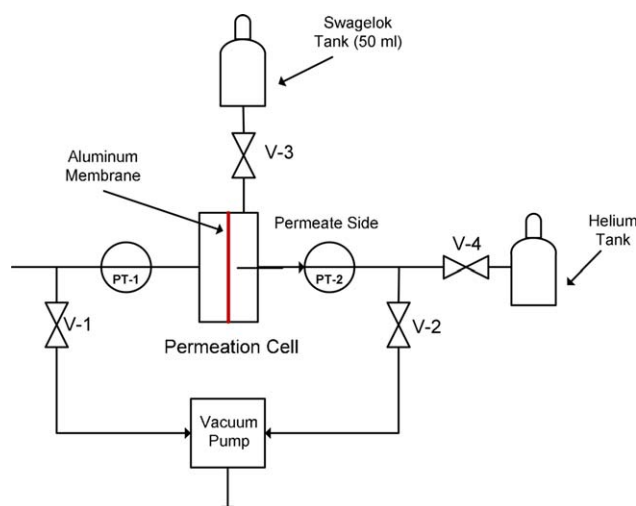
Figure 2. Schematic of the setup used to determine the permeate side volume of the permeation cell. [Color figure can be viewed in the online issue, which is available at wileyonlinelibrary.com.]

textures were observed using polarized optical microscopy (POM) using an Olympus BX51 equipped with a polarizer/analyzer, a Linkam LTS 350 hot stage and a Linkam TMS 94 temperature programmer. SAXS and WAXD experiments were performed using a Rigaku S-Max 3000 system, equipped with a copper rotating anode emitting X-rays with a wavelength of 0.154 nm (Cu Kα) and a Linkam Scientific Instruments hot stage and temperature controller. The calibration standard for both SAXS and WAXD was silver behenate. SAXS patterns were obtained using a 2D gas-filled multiwire, proportional counting detector. A Rigaku RAXIA-DI was used to read WAXD sample image plates. Temperature ramp rates of 10°C/min, equilibrium times of 30 min, and exposure times of 2 h were used for all SAXS and WAXD measurements.

Single gas permeation runs were performed using a constant volume–variable pressure permeation apparatus. Figure 2 depicts the setup used to determine the permeate volume of the membrane apparatus. An impermeable aluminum membrane was placed in the membrane cell to isolate the permeate side from the feed side. Valves 1, 2, and 3 were opened to evacuate air from the system. Valves 1 and 2 were then closed and helium was introduced in the permeate side permeation cell and the 50 mL Swagelok cylinder at 1 atm, via valve 4. This cycle was done several times to ensure only helium was present in the system. The entire system was evacuated to 1 cm Hg. Valve 3 was then closed and the remainder of the system was evacuated to approximately 0.2 cm Hg. The two volumes were then equilibrated and the volume of the permeate side was determined through a mass balance using the ideal gas law.

Membrane permeability was determined using the following relationship:

$$P = \frac{N_{A1}}{p_2 - p_1} \tag{1}$$

P is the permeability $(10^{-10}\ (cm^3\ O_2)\ cm)/(cm^2\ s\ cm\ Hg)$, N_A is the gas flux across the membrane, l is the membrane
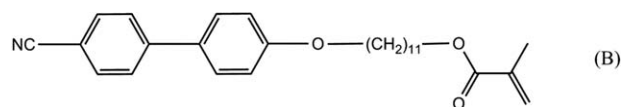

Figure 3. Monomer synthesized for use in the preparation of LCPs: 11-(4-cyanobiphenyl-4′-yloxy)undecyl methacrylate (B).

thickness, and p_2 and p_1 are the feed and permeation pressures, respectively. The permeability can be related to the diffusivity and the solubility:

$$P = DS \tag{2}$$

where D and S are the diffusivity $(10^{-8}\ cm^2/s)$ and solubility $(10^{-4}\ cm^3\ @STP/(cm^3\ cm\ Hg))$ of a gas in the membrane.

SYNTHESIS AND CHARACTERIZATION

Methacrylate monomer containing biphenyl (B), as depicted in Figure 3, was synthesized for use in the preparation of linear LCPs.

Synthesis of Liquid Crystal Monomer B
There should be a flexible spacer in side chains between the rigid mesogen and the polymer backbone, decoupling the motions of the rigid unit from the motions of the polymer main chain. The mesogens require a long spacer for a well-developed and stable mesophases. Monomer B was synthesized using a two-step synthesis of a Williamson reaction and esterification, depicted schematically in Figure 4.

Synthesis of 4′-(11-hydroxy-undecyloxy)-4-biphenylcarbonitrile (1). 5.8 g of 4′-hydroxy-4-biphenylcarbonitrile (30 mmol), 11.3 g of 11-bromo-1-undecanol (45 mmol), and 8.0 g of annealed K₂CO₃ (60 mmol) were added to 150 mL of acetone. The solution was bubbled with nitrogen for several minutes, sealed, and heated to reflux for 72 h. After cooling to room temperature, the solid present in the solution was filtered off.
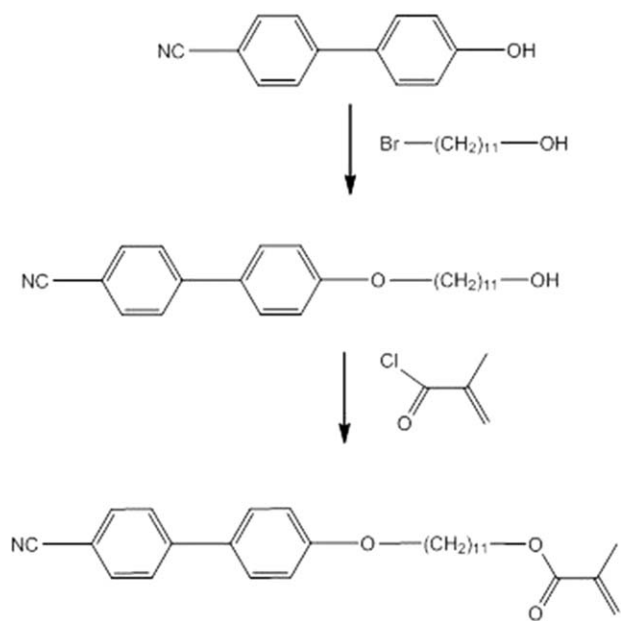

Figure 4. Reaction scheme for the preparation of 11-(4-cyanobiphenyl-4′-yloxy)undecyl methacrylate (monomer B).

Table I. Main Characteristics of the Synthesized Polymers

Sample	F_{LC}[a]	f_{LC}[b]	$M_n \times 10^{-4}$[c]	M_W/M_n[c]
Poly(2-EHA)	0.00	0.00	1.2	3.5
B-33	0.33	0.19 (0.24[d])	2.5	3.3
B-50	0.50	0.36 (0.42[d])	2.8	2.9
B-75	0.75	0.66 (0.68[d])	2.7	2.6
B-100	1.00	1.00	2.8	2.3

[a] Mole fraction of mesogenic monomer in the feed.
[b] Mole fraction of mesogenic monomer units in the (co)polymer, estimated from ^{1}H-NMR.
[c] Determined from SEC using PMMA as a standard (g/mol).
[d] Mole fraction of LC comonomer content in the sample, estimated from elemental analysis.

The solvent in the filtrate was removed under reduced pressure. The resulting solid was recrystallized several times in heptane. M.p. 98–100°C, yield—43%. ^{1}H-NMR data (300 MHz, CDCl$_3$): 7.58 (dd,4H, ortho, meta to —CN), 7.46 (d, 2H, meta to alkoxy), 6.92 (d, 2H, ortho to alkoxy), 3.93 (t, 2H, Ph—O—CH$_2$—), 3.58 (q, 2H, —CH$_2$—OH), 1.79 (qui, 2H, —O—CH$_2$—CH$_2$—), 1.19 to 1.56 (m, 16H, aliphatic).

Synthesis of 11-(4-cyanobiphenyl-4′-yloxy)undecyl methacrylate (B). 2.0 g of (1) (5.5 mmol) and 830 μL of triethylamine (6 mmol) were dissolved in 20 mL of dry THF. The solution was cooled to −5°C using ethanol and dry ice. 0.8 mL of a freshly distilled methacryloyl chloride (8 mmol) in 5 mL of THF was added dropwise to the solution. The solution was stirred at a temperature between 0 and 5°C for several hours followed by several days at room temperature to ensure the reaction was complete. Solid triethylammonium chloride was filtered off and the solvent in the filtrate was removed under reduced pressure. The resulting solid was recrystallized several times in methanol. M.p. 75–77°C, yield—63%. ^{1}H-NMR data (300 MHz, CDCl$_3$): 7.58 (dd, 4H, ortho, meta to —CN), 7.46 (d, 2H, meta to alkoxy), 6.92 (d, 2H, ortho to alkoxy), 5.48 and 6.04 (s + s, 2H, CH$_2$=C(CH$_3$)—), 3.93 (t, 2H, Ph—O—CH$_2$—), 3.58 (q, 2H, —CH$_2$—OH), 1.79 (qui, 2H, —O—CH$_2$—CH$_2$—), 1.19 to 1.56 (m, 16H, aliphatic).

Preparation of Copolymers of 2-EHA with B
Monomer B, 2-EHA, and AIBN were dissolved in toluene and poured into an ampule. The concentration of monomer B varied from 0 to 0.9 g per mL of toluene, but the total amount of acrylate and methacrylate stayed constant at 2.5 mmol/mL of toluene. The initial molar ratio of AIBN to the comonomers was 1.5×10^{-2}. The solution was bubbled and blanketed with nitrogen for several minutes and then the ampule was immediately sealed. The ampule was heated to 80°C for 48 h to induce polymerization. The resulting viscous solution was reprecipitated several times in a methanol/THF mixture (decreasing solvent ratio with increasing B ratio with respect to 2-EHA) and dried under vacuum overnight at a temperature of 80°C.

The structure and composition of the resulting (co)polymers was determined using ^{1}H-NMR and elemental analysis. Number-average molecular weights and dispersity of these materials were estimated by SEC.

Preparation of a Liquid Crystal Polymer Membrane
Polymer B-75 was sonicated for 1 h in chloroform at a concentration of 75 mg per mL of chloroform. The resulting solution was cast onto a glass substrate. The solvent was allowed to evaporate over 48 h. The cast membrane was removed using distilled water as a lubricant and the approximate thickness was 200 μm The membrane was then sandwiched between two porous PTFE supports with 0.45 μm diameter pores. The sandwiched membrane was annealed at 95°C under vacuum for 48 h. To avoid hysteresis the temperature was cooled back to room temperature at a rate of 5°C/min. The membrane was then masked with aluminum tape and placed in a permeation cell. The membrane and permeation cell were degassed for 5 h between each permeation experiment.

RESULTS AND DISCUSSION

Characterization of the Synthesized Polymers
B/2-EHA copolymers were synthesized by a free radical polymerization method. The initial ration of the mesogenic monomer to the nonmesogenic comonomer (2-EHA) in the feed varied from 0 to 1. The final mesogen fractions, molecular weights and dispersities are reported in Table I.
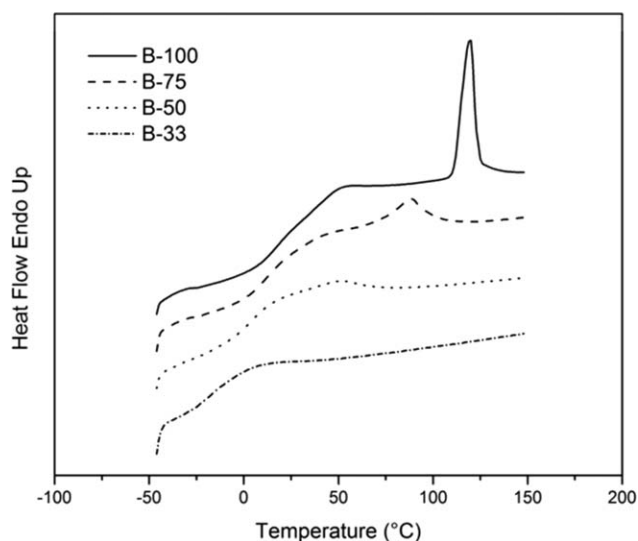

Figure 5. DSC curves of polymers containing LC comonomer B. Heating run: 10°C/min.

Table II. DSC Data for Polymers Containing 2-EHA and LC Comonomer B

Sample	Run	T^g (°C)	Δc^p (J/g ×°C)	T^m (°C)	ΔH (J/g)
Poly(2-EHA)	H	−46.0	0.05		
	C	−51.9	0.06		
B-33	H	−15.7	0.39		
	C	−23.9	0.27		
B-50	H	4.6	0.58	50.3	2.4
	C	−9.4	0.53	37.2	−0.92
B-75	H	11.9	0.61	88.8	5.9
	C	1.1	0.60	79.2	−6.3
B-100	H	17.8	0.93	111.3	12.4
	C	7.9	0.91	111.7	−13.1

Heating/cooling rate was 10°C/min: T_m, mesophase to isotropic transition temperature.

As expected, the fraction of mesogenic comonomer units incorporated into the copolymer increased with the increasing mesogenic comonomer content in the feed. The values found using NMR are in a relatively good agreement with those from elemental analysis. All the homopolymers and copolymers exhibited a unimodal distribution of molecular weights. The ratio M_w/M_n found for these polymers varied from 2.3 to 3.5. This is in accordance with the nature of the free radical polymerization process.[14] The presence of the mesogenic comonomer in the feed contributed to a significantly narrower molecular weight distribution in the resulting polymer in comparison to the neat non-LC homopolymer poly(2-EHA) ($M_w/M_n = 3.5$). This is to be attributed to a decrease in the overall reaction rate caused by the addition of the bulky biphenyl containing monomers.

Phase Behavior
Thermal properties of the preparedhomopolymer and copolymers were determined using differential scanning calorimetry, polarized optical microscopy, and X-ray scattering.

Differential Scanning Calorimetry (DSC). As expected, only the homopolymer poly(2-EHA) exhibited a simple thermal behavior with one glass transition.[15] The values found for this transition ($T_g \sim -50$°C and $\Delta c_p \sim 0.05$ J/g × °C) are typical for amorphous polymers.[16]

DSC curves for polymers containing mesogenic comonomer B and 2-EHA are depicted in Figure 5. The associated DSC data are summarized in Table II.

Incorparation of B into the polymer chains dramatically influenced the thermal behavior of the resulting polymer. The temperature and Δc_p of glass transition of the B/2-EHA polymers increased with increasing B content, from −46°C and 0.05 J/g × °C for the homopolymer poly(2-EHA) up to 18°C and 0.93 J/g × °C for the homopolymer B-100. Polymer samples containing more than 19 mol % B exhibited a peak that can be connected with a mesophase/isotropic state transition. As the content of B increases, the peak shifts to higher temperatures and the change in enthalpy increases. Thus the thermal stability of the mesophase increases with the mesogenic monomer content. For the copolymer B-50, the width of the temperature interval of the mesophase is ∼45°C, whereas in the homopolymer B-100, the mesophase is stable over an interval of ∼100°C. In addition, the difference in isotropic state/mesophase transition peak position between heating and cooling decreased as B content increased.

Polarizing Optical Microscopy (POM)
POM was employed to confirm results obtained from DSC and to determine the optical textures of the LC samples. Heating and cooling rates were 10°C/min. The heating/cooling was
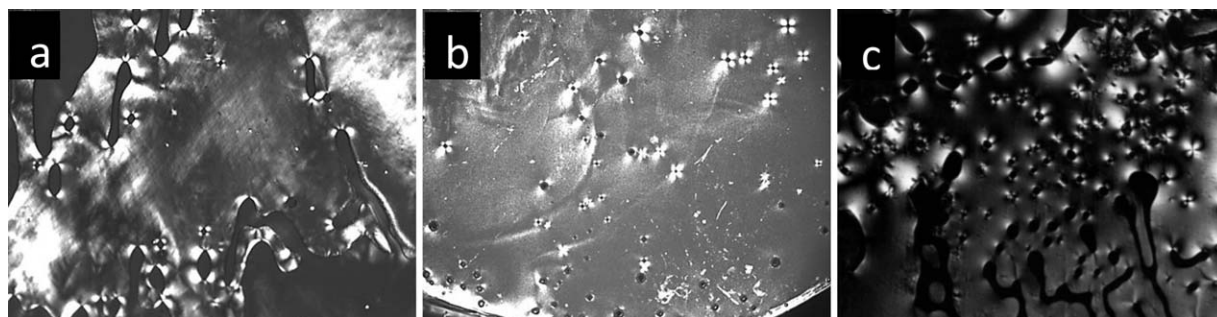

Figure 6. POM images of samples: (a) B-50 at 40°C, (b) B-75 at 60°C, (c) B-100 at 80°C. Cooling rate 10°C/min. The width of the image is about 400 µm.

Table III. Thickness of the Mesophase Layer (d_{LC}) and Average Distance between Mesogen Units Envolved in the Mesophase (D_{LC}) for B-Polymers (30°C, Cooling Rate 10°C/min)

Sample	d_{LC} (Å)	D_{LC} (Å)
B 50	54.6	4.8
B 75	49.7 (24.7)	4.6
B 100	47.1 (23.2)	4.5

Table IV. Permeability, Diffusion, and Solubility for Membrane B-75

	Permeability (barrer)	Diffusivity (10^{-8} cm^2/s)	Solubility [10^{-4} cm^3 @ STP/cm^3 cm Hg)]
CH_4	4.7	252	1.9
CO_2	61.0	151	40.5
Propane	3.3	14	22.9
Propylene	25.2	55	45.7
O_2	20.1	486	4.1
N_2	7.0	223	3.2

stopped at various temperatures to allow the material to equilibrate prior to images being taken.

POM images for B/2-EHA copolymers are shown in Figure 6. The cyanogroup present in the B comonomers possesses a strong dipole moment, suggesting that the formation of a smectic mesophase with a bilayered structure is preferred.[17] Schlieren textures observed for polymers B-50, B-75, and B-100 exhibited singularities of ±1, in accordance with the assumption of a smectic mesophase. The smectic mesophase was also confirmed via X-ray diffraction (see X-ray Scattering). The temperature intervals over which the mesophase was stable broadened with increasing B content, in agreement with the DSC results.

X-ray Scattering

X-ray results for B-polymers with high content of LC comonomer are summarized in Table III. Data were collected at 30°C during cooling. A mesophase was found in all the measured samples at this temperature. The effective thickness of the layered structure was calculated from the first order peak (d_{LC}). The distance calculated from second order peak is shown in

brackets. The thickness of the smectic bilayer decreased from 54.6 (B-50) to 49.7 Å (B-75) and 47.1 Å (B-100) as the mesogen content increased. The significantly lower value of the effective bilayer thickness in the homopolymer compared to the theoretical value for extended chains (49.8 Å) could be explained by the appearance of a smectic C bilayer with tilted mesogenic units. The average distance between mesogens in the mesophase (D_{LC}) also decreased with increasing mesogen content from 4.8 Å (B-50) to 4.5 (B-100). This suggests that the increasing mesogen content results in a more ordered structure.

Diffractograms of the copolymer B-75 are shown in Figure 7. In the isotropic state (110°C), only a broad diffuse peak is observed corresponding to a distance of 4.9 Å. At 60°C, when the polymer exhibits a LC mesophase, the position of the wide-angle maximum corresponds to an average distance between mesogens of 4.6 Å. In the small-angle region, two sharp reflections are observed at 49.7 (first order) and 24.7 Å (second order). The maximum at 49.7 Å is lower than the theoretical value calculated for the thickness of the smectic A bilayer (54.3 Å). The significantly lower value of the effective bilayer thickness compared to the theoretical value for extended chains could be explained by the appearance of a smectic C bilayer with tilted mesogenic units. Within this bilayer the mesogens
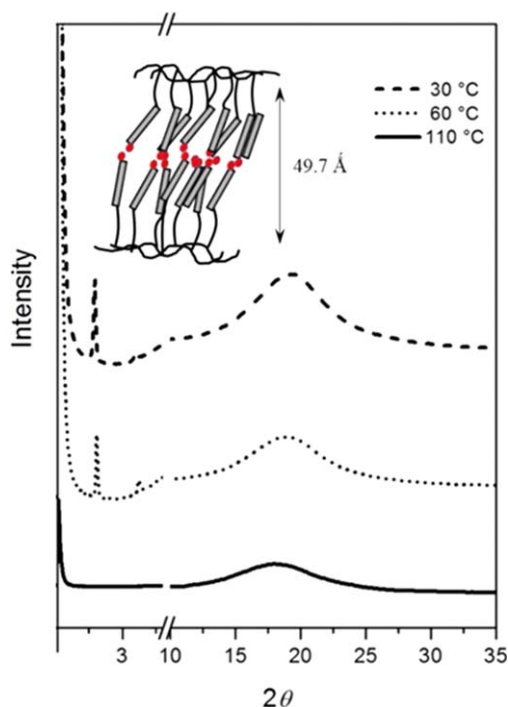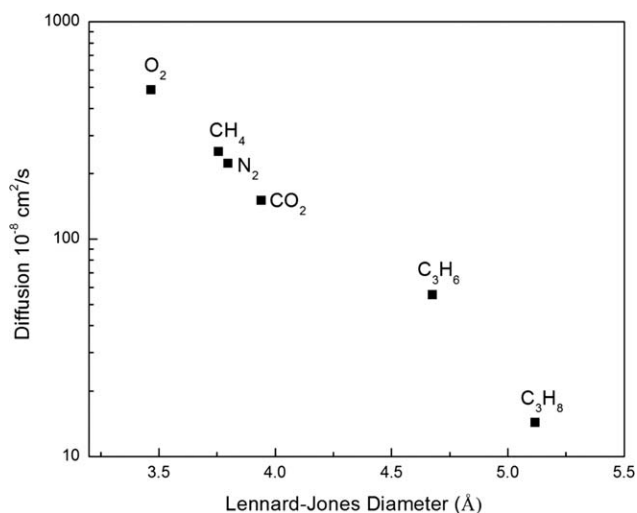

Figure 7. Temperature development of the X-ray diffractograms for sample B-75. Cooling rate 10°C/min. [Color figure can be viewed in the online issue, which is available at wileyonlinelibrary.com.]

Figure 8. Diffusion coefficient of permeant gases with respect to Lennard–Jones Diameter.

Table V. Permeability, Diffusion, and Solubility Selectivity Coefficients for Membrane B-75

	CO_2/CH_4	Propylene/ Propane	O_2/N_2
Permeability selectivity	12.9	7.7	2.9
Diffusion selectivity	0.6	3.9	2.2
Solubility selectivity	21.7	2.1	1.3

are tilted and oriented in an antiparallel arrangement, and strong interactions between polar cyano groups takes place. A schematic of the mesophase structure is presented in Figure 7.
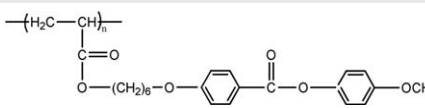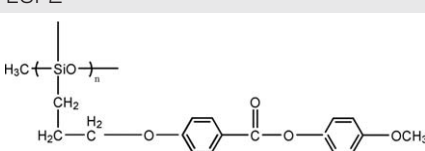
PRELIMINARY GAS PERMEABILITY MEASUREMENTS

Preliminary single gas permeation measurements were performed for gases CH_4, CO_2, propane, propylene, O_2, and N_2 with the membrane B-75. In order to understand the gas permeation mechanism through liquid crystal polymers, it is useful to compare the diffusion and solubility behavior of each gas. The diffusion coefficient for the gases was determined using the time lag approach. The solubility of the gases was then calculated using eq. 2. Runs were performed at 23°C and at a feed pressure of 2 atm. The membrane thickness was approximately 200 μm.

As shown in Table IV, the trend in the permeability of the gases in B-75 is, in decreasing order, CO_2 > propylene > O_2 > N_2 > CH_4 > propane. Diffusion is dependent on the molecular diameter of the permeant gases. For larger gases (CO_2, propane, and propylene), kinetic diameter breaks down as a useful scaling parameter for penetrant size [18]. Thus, Lennard–Jones diameter is more appropriate for correlating molecular sizes to diffusion coefficients for this group of constituents. As can be seen in Figure 8, diffusion coefficients for all gases decreased with increasing Lennard–Jones diameter, which is typical behavior for both rubbery and glassy polymers.

Selectivities calculated for gas pairs CO_2/CH_4, propylene/propane and O_2/N_2 are shown in Table V. Membrane B-75 exhibited a CO_2/CH_4 permeability selectivity of approximately 12.9 which was dominated by a large solubility selectivity of 21.7. This is likely due to interactions occurring between the quadrupole of CO_2 and the polar LC mesogens. Propylene/propane exhibited a permeability selectivity of 7.7 and had contributions from both diffusion (3.9) and solubility (2.1) selectivity. The diffusion selectivity is due to the difference in diameter, while the solubility selectivity is likely due to interactions between the slightly polar double bond in the propylene molecule and the polar mesogens. The permeability selectivity of 2.9 for O_2/N_2 gas pair was almost entirely due to the difference in the diffusion coefficients caused by the difference in size.

Table VI. Comparison of Permeabilities and Permeability Selectivities of the Side Chain Liquid Crystal Copolymer B-75 with Those of Homopolymers LCP1[8] and LCP2[13]

	PO_2[a]	PN_2[a]	PCO_2	PCH_4	$\frac{PO_2a}{PN_2}$	$\frac{PCO_2}{PCH_4}$
LCP1	1.65	0.329	7.61	0.65	5.02	11.7
LCP2	1.75	0.38	11.1	0.65	4.6	16.9
B-75	20.1	7.0	61.0	4.7	2.9	12.9

[a] Numerical values in 10^{-10} cm^3 @STP cm/(cm^2 s cm Hg).

Table VII. Comparison of Solubilities and Diffusivities and Solubility and Diffusivity Selectivities of the Side Chain Liquid Crystal Copolymer B-75 with those of Homopolymers LCP1 and LCP2

	DO_2[a]	DCO_2[a]	SO_2[b]	SCO_2[b]	$\frac{D_{O_2}}{D_{N_2}}$	$\frac{D_{CO_2}}{D_{CH_4}}$	$\frac{S_{O_2}}{S_{N_2}}$	$\frac{S_{CO_2}}{S_{CH_4}}$
LCP1	3.81	1.83	4.33	41.6	1.66	0.8	3.0	13.8
LCP2	3.85	1.77	4.54	61.6	2.39	1.2	1.9	17.7
B-75	48.6	15.1	4.13	40.5	2.2	0.6	1.3	21.7

[a] Numerical values in 10^{-7} cm^2/s.
[b] Numerical values in 10^{-4} cm^3 @STP/(cm^3 cm Hg).

In order to understand the influence of LCP properties on gas transport, it is useful to compare B-75 with other LCPs. The gas transport properties of the B-75 copolymer membrane is compared to those of two previously reported side-chain liquid crystal homopolymers based on a 4-methoxyphenyl-benzoatemesogenic side group attached to a polyacrylate backbone (LCP1)[8] or a polysiloxane backbone (LCP2).[13] Both LC homopolymers were tested at 25°C and contained no non-LC comonomers. At this temperature, LCP1 exhibits a smectic mesophase while LCP2 exhibits a nematic mesophase.

As shown on Table VI, the permeability coefficients of O_2, N_2, CO_2, and CH_4 in the B-75 membrane are approximately one order of magnitude higher than in either the LCP1 or LCP2 homopolymer membranes. Table VII reports solubilities, diffusivities, solubility selectivities, and diffusivity selectivities for B-75, LCP1, and LCP2. Solubilities and solubility selectivities for membrane B-75 were of the same order of magnitude as LCP1 and LCP2. The higher gas permeabilities were the result of higher diffusion coefficients. It has previously been suggested that it is not the polymer backbone, but the pendant groups that play the most important role on the gas transport through LCP films.[8] These results indicate that the addition of a non-LC comonomer could enhance gas transport performance by increasing mesogenic and backbone intersegmental mobility with little trade-off in selectivity. This behavior is in our interest and we will be further investigating this phenomenon in the future.

CONCLUSIONS

Methacrylate monomer containing a cyanobiphenyl (B) group as the rigid mesogen was synthesized and characterized. Copolymers of B with 2-EHA prepared by free radical copolymerization were characterized by NMR and SEC methods. Liquid crystalline mesophases were observed in copolymers containing at least 36 mol % of B. Based on POM and X-ray scattering, the mesophases were identified as smectic bilayer. Increasing mesogenic comonomer content also lead to a broadening of the temperature intervals over which the LC mesophases were stable. A liquid crystal polymer membrane containing cyanobiphenyl was successfully fabricated in order to examine gas transport behavior. Our preliminary measurements suggest that the use of ordered polar mesogens in polymer membranes may be a valid strategy for performing or enhancing gas separations.

REFERENCES

1. Devi, R. *IJRRA* **2015**, *2*, 18.
2. Rasing, T.; Musevic, I. Surfaces and Interfaces of Liquid Crystals; Springer: Berlin, **2013**.
3. Barbero, G.; Evangelista, L. R. Adsorption Phenomena and Anchoring Energy in Nematic Liquid Crystals; CRC Press: Boca Raton, **2005**.
4. Blumstein, A. Polymeric Liquid Crystals; Springer: Berlin, **2013**.
5. Ujiie, S.; Miyazaki, W.; Iimura, K. *Polym. J.* **2012**, *44*, 561.
6. Hu, T.; Yi, J.; Xiao, J.; Zhang, H. *Polym. J.* **2010**, *42*, 752.
7. Chen, D.-S.; Hsiue, G.-H.; Hsu, C.-S. *Die Makromol. Chem.* **1991**, *192*, 2021.
8. Chen, D.-S.; Hsiue, G.-H.; Hsu, C.-S. *Die Makromol. Chem.* **1992**, *193*, 1469.
9. Kawakami, H. *J. Membr. Sci.* **1997**, *133*, 245.
10. Głowacki, E.; Horovitz, K.; Tang, C. T.; Marshall, K. L. *Adv. Funct. Mater.* **2010**, *20*, 2778.
11. Rao, H.; Zhang, Z. *J. Appl. Polym. Sci.* **2012**, *123*, 191.
12. Poláková, L.; Sedláková, Z.; Beneš, H.; Valentová, H.; Krakovský, I.; Rabie, F. *J. Rheol.* **2013**, *57*, 1297.
13. Chen, D.-S.; Hsiue, G.-H. *Die Makromol. Chem.* **1993**, *194*, 2025.
14. Liu, X.; Jing, Y.; Bai, Y. *Front. Chem. China* **2008**, *3*,41.
15. Shojaei, A. H.; Paulson, J.; Honary, S. *J. Control. Release* **2000**, *67*, 223.
16. Menczel, J. D.; Prime, R. B. Thermal Analysis of Polymers: Fundamentals and Applications; Wiley: New York, **2014**.
17. Barny, L. P.; Dubols, J.-C.; Friedrich, C.; Noël, C. *Polym. Bull.* **1986**, *15*, 341.
18. Freeman, B.; Yampolskii, Y.; Pinnau, I. Materials Science of Membranes for Gas and Vapor Separation; Wiley: New York, **2006**.